

Green synthesis of Fe₂O₃ nanoparticles using *Piper betle* leaf and its characterization

Toijam Suma Chanu¹, K. Nomita Devi¹

¹(Department of Physics, Manipur University, India)

Corresponding Author: Toijam Suma Chanu

Abstract: Iron oxide (Fe₂O₃) nanoparticle was successfully synthesized by using cost effective and eco-friendly green method assisted by leaf extract of *Piper betle*. The synthesized sample was characterized by using X-ray diffraction (XRD), Scanning electron microscope (SEM), Energy dispersive X-ray Spectroscopy (EDAX), UV-vis Spectrophotometer, Fourier transform Infra-red spectroscopy (FTIR) and LCR meter. XRD confirms the formation of pure rhombohedral phase of Fe₂O₃. The lattice parameters and crystallite size of the synthesized sample were found to be 66.22 nm, a=b=0.5395 nm and c=1.388 nm. The surface morphology of the synthesized sample was revealed by SEM image, EDAX spectrum shows the presence of light element K, Cl and Mg in addition to Fe and O in the synthesized sample. The band gap energy calculated from the UV-vis absorption spectrum is found to be 2.6 eV. FTIR study confirms the presence of Fe-O stretching vibration. The frequency dependent dielectric properties of the synthesized sample was measured by LCR meter in the frequency range of 100 Hz to 1 MHz which shows the typical frequency dispersion. The temperature dependent dielectric property and the ac electrical conductivity of the synthesized sample was studied and the results obtained were analyzed. The magnetic study of the synthesized sample shows the ferromagnetic behavior.

Date of Submission: 01-11-2018

Date of acceptance: 15-11-2018

I. Introduction

Magnetic nanoparticles have attracted wide research interest because of their potential application in information storage, color imaging, high density magnetic storage media, magnetic refrigerator, gas sensing, ferrofluids, catalysis, medical diagnostic etc.¹⁻⁴ Among the various magnetic iron oxide nanoparticles, Fe₂O₃ nanoparticle has wide range of advantage due to its high electrical resistivity, low eddy current loss^{5,6}. They are widely used in many ferrites devices and in production of electronic and magnetic components, converters and electromagnetic wave absorbers⁷. There are various methods used in the preparation of Fe₂O₃ nanoparticles such as hydrothermal method, sol gel method, co-precipitation method, auto combustion method, green synthesis method etc⁸⁻¹⁵. Green synthesis method is one of the most convenient technique to synthesize the Fe₂O₃ nanoparticles because of its cost effectiveness, environmental friendliness, easily sealed up for large scale synthesis and in this method there is no need to use high pressure, energy, temperature and toxic chemicals. In the present work, Fe₂O₃ nanoparticle have been synthesized by economical and environment friendly green synthesis method using betel leaf extract. A detailed structural, optical, electrical and magnetic characterization of the synthesized sample have been carried out.

II. Material And Methods

Materials Required

For the synthesis of Fe₂O₃ nanoparticles *Piper betle* leaf extract was used as a reducing agent. The ferric nitrate Fe(NO₃)₃·9H₂O which was used as a precursor material for Fe²⁺ ions was procured from LobaChemie. Whatmann filter paper No. 1 grade 42 was used for the filtration and Narang scientific work (NSW-142) heating Oven was used for the drying process.

Preparation of *Piper betle* leaf (betel) extract

Fresh leaves of *Piper betle* were thoroughly washed with running tap water followed by distilled water. The washed leaves was then boiled with distilled water in a glass beaker until the colour changes to greenish yellow. The leaf extract was cooled at room temperature and filtered using filter paper.

Green Synthesis of Fe₂O₃ nanoparticles

Appropriate amount of Fe(NO₃)₃·9H₂O was dissolved in 400 ml of *Piper betle* leaf extract to make 0.1 M solution of Fe(NO₃)₃·9H₂O. The mixed solution was stirred for 1 hr in a magnetic stirrer at 600 rpm to make the solution homogenous. The homogenous solution was heated in a heating mantle at 350°C until combustion

takes place. The reddish ash powder obtained after complete combustion was washed several times with distilled water to remove the impurities and dried in a hot plate at 200°C. The dried powder was ground using an agate mortar to obtain the fine powder.

Characterization

The structural properties of the green synthesized Fe₂O₃ nanoparticle was characterized by using Phillip's PANalytical X'Pert PRO diffractometer with Cu target ($\lambda=1.5405\text{\AA}$) in the 2θ range of 20°-80°. The XRD pattern was analyzed using X-pert Highscore Plus and data was compared with ICDD/PDF2 database. The surface morphology and elemental analysis of the synthesized sample was examined by scanning electron microscope (SEM) (FEI QUANTA 250) equipped with energy dispersive X-ray (EDAX) spectrometer (EDAX QUANTA 250). The optical absorption spectrum of the synthesized sample was recorded by UV-vis spectrophotometer (Ocean Optics HR4000) in the wavelength range of 350nm-700nm. FTIR spectrum of the synthesized sample was recorded over the range of 400-4000 cm⁻¹ in a FTIR spectrometer (SHIMADSU 8400S). Pelletized sample was used for the dielectric measurement by LCR meter (HP 4284A) as a function of frequency from 100Hz-1MHz and temperature in the range from 20°C-155°C. In order to obtain good electrical contact silver paste was painted on the polished sintered surface of the pellet. The magnetic property was characterized by VSM (Vibrating sample magnetometer).

III. Result and Discussion

Fig 1 shows the XRD pattern of Fe₂O₃ nanoparticle. The X-ray diffraction peaks were obtained at 24°, 33°, 35°, 40°, 49°, 54°, 62°, 63° and 75° corresponding to the planes (012), (104), (110), (113), (024), (116), (122), (214), (300) and (220). The XRD pattern confirms the formation of pure rhombohedral phase of Fe₂O₃ nanoparticles which is in good agreement with ICDD/PDF2 database 00-24-0072. The crystallite size was calculated from the most prominent peak using the Debye Scherrer formula (eqn (1)) and was found to be 66nm.

$$g = \frac{0.9\lambda}{\beta \cos \theta} \quad (1)$$

where, g is the crystallite size, λ is the wavelength of X-ray radiation, β is the full width at half maximum (FWHM), θ is the Bragg's angle.

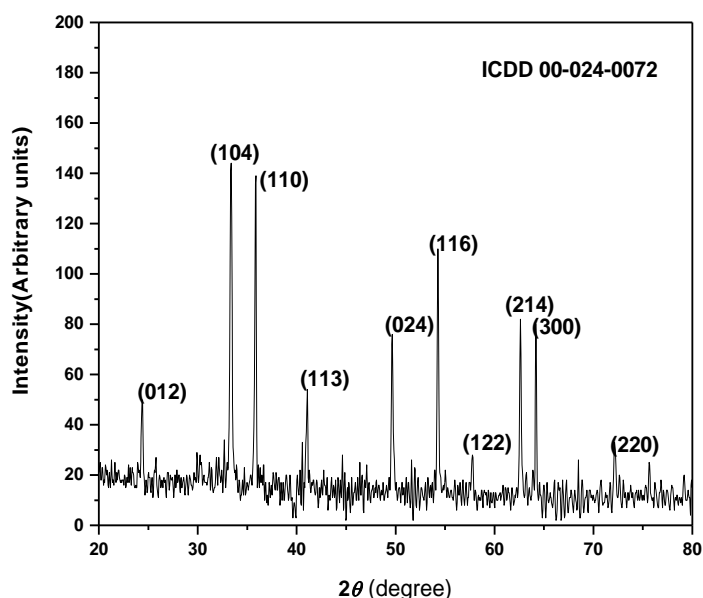


Fig.1 XRD pattern of Fe₂O₃ nanoparticle.

As the Fe₂O₃ nanoparticles crystallized in rhombohedral form, its lattice parameter and cell volume were calculated by using the formula

$$\frac{1}{d^2} = \frac{4}{3} \left(\frac{h^2 + hk + k^2}{a^2} \right) + \frac{l^2}{c^2} \quad (2)$$

and cell volume, $V = \frac{\sqrt{3}}{2} a^2 c$ (3)

where h, k, l are the miller indices and a, b, c are the lattice parameter. The lattice parameter and cell volume were found to be $a=b=0.503$ nm, $c=1.377$ nm and $V=0.303$ (nm)³ which were well matched to the standard value determined by ICDD reference no.00-024-0072.

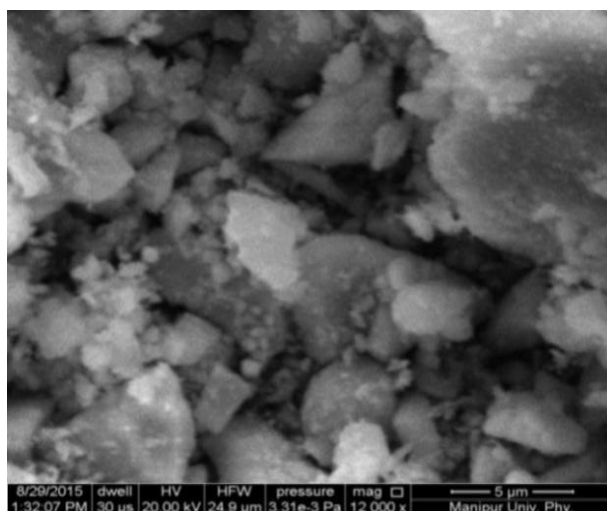


Fig 2: SEM image of Fe₂O₃ nanoparticle.

Fig 2 shows the SEM image of the synthesized Fe₂O₃ nanoparticle. It is observed that the particles were highly agglomerated. Some distorted spherical shape particles is also seen in the image.

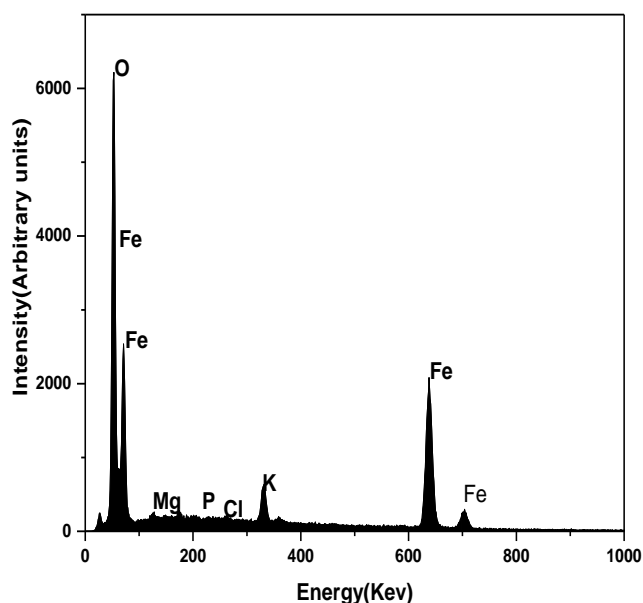


Fig 3: EDAX spectrum of Fe₂O₃ nanoparticle

Fig 3 shows the EDAX spectrum of the synthesized Fe₂O₃ nanoparticle. The spectrum shows the presence of light elements K, Mg, Cl in addition to Fe and O. These light elements are present in high amount in plants and its detection in the sample might had been from the leaf extract that was used during the synthesis process¹⁶.

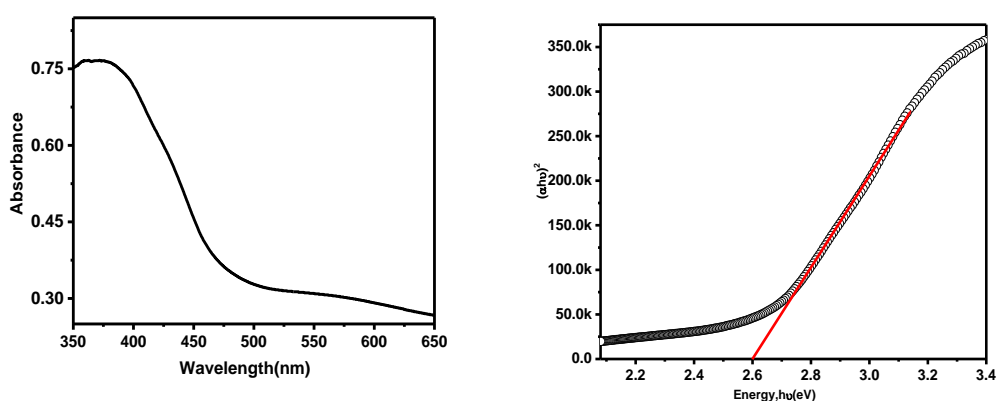


Fig.4(a) UV-vis absorbance spectrum of Fe₂O₃ nanoparticle (b) Tauc plot of Fe₂O₃ nanoparticle

The direct band gap energy of the synthesized sample can be calculated from the absorption spectrum by using the Tauc relation given below

$$\alpha h\nu = c(h\nu - E_g)^n \quad (4)$$

where $\alpha = 2.303A/t$ is the absorption co-efficient, A is the absorbance, t is the thickness, C is the proportionality constant, E_g is the band gap and $h\nu$ is the photon energy. The value of band gap energy calculated from the Tauc plot is found to be 2.6 eV which is in good agreement with the value (~2.67 eV) reported by P. Mallick et.al¹⁷.

Fig 5 shows the FTIR spectrum of Fe₂O₃ nanoparticle. The absorption band at 3404 cm⁻¹ is due to the O-H stretching vibration mode of adsorbed water. The band at 2911 cm⁻¹, 1380 cm⁻¹ and 1000 cm⁻¹ are attributed to C-H and C-O bond. The strong band at 538 cm⁻¹ and 456 cm⁻¹ are attributed to the Fe-O stretching vibration.

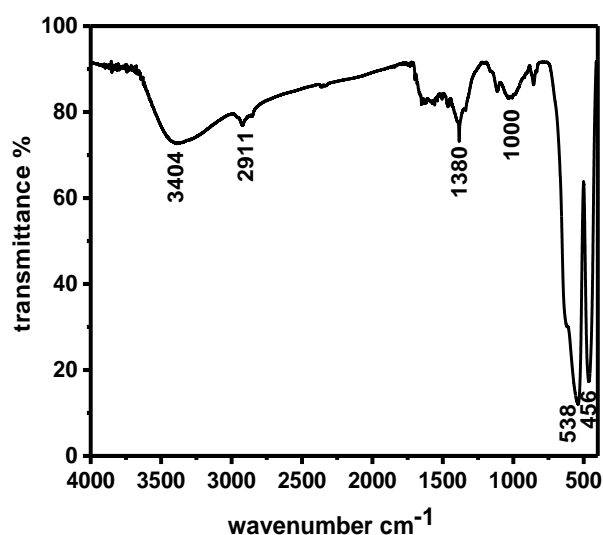


Fig.5 FTIR of Fe₂O₃ nanoparticles.

Fig 6(a) displays the variation of dielectric constant as a function of frequency at room temperature from 100 Hz to 1 MHz. From the graph it is observed that the dielectric constant decreases steeply at lower frequency and remain constant at higher frequencies indicating the usual frequency dispersion. When an electric field is applied within dielectric material orientational polarization and space charge polarization takes place within it¹⁸⁻²². At lower frequencies, the dipoles within the material can orient themselves to respond to the applied field and accumulation of charges takes place at the grain boundaries which results in the high value of dielectric constant. However, with further increase in frequencies, a point is reached where the dipoles do not orient themselves with the direction of applied field, so polarization cannot achieve its saturation value and

hence a decrease in dielectric constant is observed at higher frequencies.

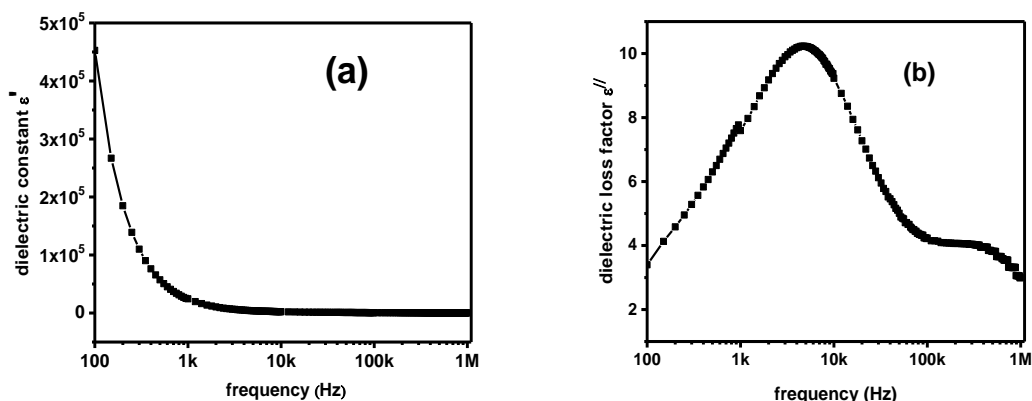


Fig.6 Variation of (a) dielectric constant with frequency (b) dielectric loss with frequency of Fe_2O_3 nanoparticles.

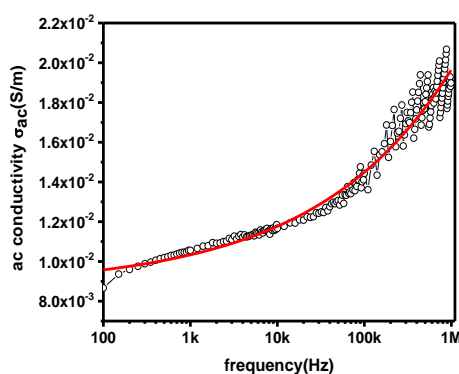


Fig.7 Variation of ac conductivity with frequency of Fe_2O_3 nanoparticle

Fig 7 displays the variation of ac conductivity as a function of frequency at room temperature from 100 Hz to 1 MHz. From the graph it is observed that at low frequency range the ac conductivity is nearly independent of the frequency and had been attributed to the dc conductivity of the sample. With the increasing frequency, the ac conductivity increases obeying the Jonsher's Universal power law $\sigma_{ac} = \sigma_{dc} + A\omega^n$,^[23] where σ_{dc} is the dc conductivity (frequency independent plateau in the low frequency region), A is a constant and n is a characteristic parameter ($0 < n < 1$). The curves is not well fitted at lower frequency region due to the electrode polarisation effect along with the dc conductivity, however, the curves is well fitted at the higher frequency range confirming the frequencydependence of ac conductivity. The frequency dependence of ac conductivity is related with the conduction by the electron hopping within the dielectric material. At lower frequencies the grain boundaries are more active and hence the hopping between dielectric is less. As the frequencies of the applied field increases, the conductive grains become more active thereby promoting the hopping within dielectric material which results high ac conductivity. Therefore a gradual increase in conductivity with frequency is observed.

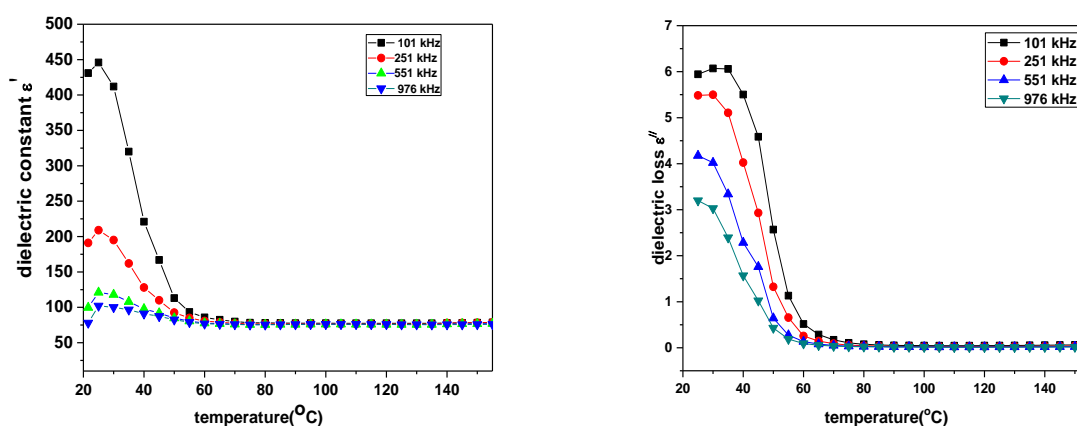


Fig.8 Variation of (a)dielectric constant with temperature (b) dielectric loss with temperature of Fe₂O₃ nanoparticles.

Fig 8 (a) and (b) displays the variation of dielectric properties with temperature. From the graph it is observed that dielectric constant slowly increase upto 25°C then decreases steeply and remains constant at higher temperature. This may be attributed to the fact that with the increase in temperature the charge at the grain boundaries can overcome the resistive barrier and conduction take place which increases the thermal oscillation however after a certain temperature disorder of dipoles takes place which results the decrease in dielectric constant indicating a phase transition²⁴⁻²⁷.

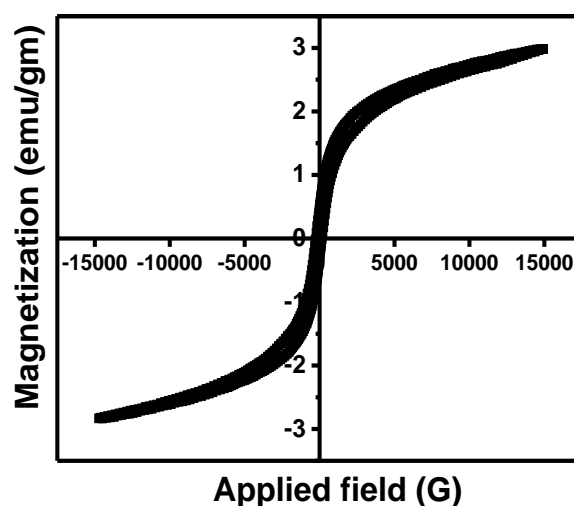


Fig. 10 Room temperature M-H loop of Fe₂O₃ nanoparticles

Figure 10 shows the variation of Magnetization M with Applied field H of Fe₂O₃ nanoparticles. From the hysteresis loop it is observed that Fe₂O₃ shows the ferromagnetic behavior with Coercivity, $H_c=216.90$ G, Magnetization, $M_s=2.9087$ emu/gm, Retentivity, $M_r=0.40377$ emu/gm and Squareness=0.13882. Similar experimental results were also obtained by the Arvish Kumar Arora et.al²⁸ which reports ferromagnetic behavior of Fe₂O₃ nanoparticles with Magnetization, $M_s=1.7$ emu/gm. The observed increase in Magnetization in the current work in comparison with the above issue to the difference in crystallite size of the sample.

IV. Conclusion

Fe₂O₃ nanoparticle was successfully synthesized by green method using the *Piper betle* leaf extract. The nanostructures of the prepared Fe₂O₃ have been confirmed by using XRD and SEM. The electrical properties were studied by the LCR meter. Morphological study shows highly agglomerated particles. EDAX spectrum shows the presence of impurity K, Mg, Cl in addition to Fe and O. From the UV-vis spectra the value of band gap energy was found to be 2.6 eV. FTIR confirms the presence of Fe-O stretching vibration. The sample shows the frequency dispersion at lower frequency and exhibit high dielectric constant. The dielectric loss factor shows the oscillating behavior and the ac conductivity shows the frequency dependence at higher frequency. The sample shows the high dielectric properties at lower temperature which decreases at higher temperature. The magnetic property of Fe₂O₃ nanoparticles shows the ferromagnetic behavior.

References

- [1]. N. A. Frey, S. Peng, K. Cheng and S. Sun. Magnetic nanoparticles: synthesis, functionalization and application in bioimaging and magnetic energy storage. *Chem. Soc. Rev.* 2009;38:2532-2542.
- [2]. P. Sun, L. You, D. Wang, Y. Sun, J. Ma, G. Lu. Synthesis and gas sensing properties of bundle like α -Fe₂O₃ nanorods. *Sensors and Actuators B.* 2011;156:368-374.
- [3]. W. Weiss, W. Ranke. Surface Chemistry and Catalysis on a well defined epitaxial iron oxide layers. *Prog. Surf. Sci.* 2002;70:1-151.
- [4]. Jordan, R. Scholz, P. Wust, H. Fahling, R.J. Felix. Magnetic fluid hyperthermia (MFH): Cancer treatment with AC magnetic field induced excitation of biocompatible superparamagnetic nanoparticles. *J. Magn. Magn. Mater.* 1999;201:413-419.
- [5]. H. Shokrollahi, K. Janghorban. Soft magnetic composite materials (SMC_s). *Journal of Materials Processing Technology* 2007;189:1-12.
- [6]. R. G. Kumar, K. V. Kumar and Y. C. Venudhar. Synthesis, Structural and Magnetic Properties of Copper Substituted Nickel ferrites by Sol gel Method. *Materials Sciences and Applications.* 2012;3:87-91.
- [7]. Xu, Y., Liang, Y.T., Jiang, L. J, Wu, H.R., Zhao, H.Z. and Xue, D.S. Preparation and Magnetic Properties of ZnFe₂O₄ Nanotubes. *Journal of Nanomaterials.* 2010; 2011:1-5.
- [8]. J. Hua, Y. HeQing. Controlled synthesis and magnetic Properties of Fe₃O₄ walnut spherical particles and octahedral microcrystal. *Sci. chin. Scr.E Tech. Sci.* 2008;51:1911-1920.
- [9]. S.M. Reda. Electric and dielectric properties of Fe₂O₃/Silica nanocomposites. *International Journal of Nanoscience and Technology.* 2013;1(5):17-28.
- [10]. D. K. Kim, Y. Zhang, W. Viot, K.V Rao, J. Kehr, B. Bjelke, M. Mohamed. Superparamagnetic iron Oxide nanoparticles for biomedical application. *Sci. Mater.* 2001;44:1713-1717.
- [11]. A. Hiremath, A. Venkataraman. Dielectric, Electrical and Infrared studies of γ -Fe₂O₃ prepared by Combustion method. *Bull. Mater. Sci.* 2003;26(4):391-396.
- [12]. S.S.Ur Rahman, M.T.Qureshi, K.Sultana et.al. Single step growth of iron oxide nanoparticles and their use as glucose biosensor. *Results in Physics.* 2017;7:4451-4456.
- [13]. M. Mahdavi, F. Namvar, M.B. Ahmad and R. Mohamad. Green Biosynthesis and Characterization of Magnetic Iron Oxide (Fe₂O₄) nanoparticles using Seaweed (*Sargassummuticum*) Aqueous extract. *Molecules.* 2013;18:5954-5964;doi:10.3390/molecules18055954.
- [14]. L. Pravallika, P. G. Krishna Mohan, K. Venkateswara. Green synthesis of iron oxide magnetic nanoparticles using *CentellaAsiatica* plant Atheranostic Agent. *International Journal of Engineering Research.* 2015;3:52-59.
- [15]. Suganya, D., Rajan, M.R and Ramesh, R.. Green synthesis of Iron Oxide nanoparticles from the leaf extract of *PassifloraFoetica* and its antibacterial activity. *International Journal of Current Research.* 2016;8:42081-42085..
- [16]. Iravani. Green synthesis of Metal nanoparticles using plants. *Green chem.* 2011;13:2638-2650.
- [17]. P. Mallick, B. N. Dash. X-ray Diffraction and UV visible characterization of α -Fe₂O₃ nanoparticles annealed at different temperature. *Nanoscience and nanotechnology.* 2013;3(5):130-134.
- [18]. Tareev B, *Physics of dielectric materials* (Mir Publishers, Moscow). 1979;51.
- [19]. D. S. Kumar, K.C. Babu Naidu, M. Mohamed rafi, et al. Structural and dielectric properties of superparamagnetic iron oxide nanoparticles (SPIONs) stabilized by sugar solutions. *Materials Science-Poland,* 2018;36(1):123-133.
- [20]. C. G. Koops, *Phy. Rev.* 1951;83(1):121-124.
- [21]. Narayan, K. B, Natarajan and Sakthivel. Biological synthesis of metal nanoparticles by microbes. *Adv. Colloid Interface Sci.* 2010;156:1-13.
- [22]. Abhilsh, Revati, K. Pandey, B.D. Microbial synthesis of iron based nanomaterials- A review. *Bull. Mater. Sci.* 2011;34:191-198.
- [23]. K. Jonsher. The 'Universal' dielectric response. *Nature.* 1977;267:673-679.
- [24]. A. Aldar, R. K Pinjiri, N. M. Burange. Electric and Dielectric behavior of Ni-Co-Cd Ferrites. *ISOR Journal of Applied Physics.* 2014;6(4):23-26.
- [25]. V. R Reddy, G. G. Mohan, D. Ravinder, B. S. Boyanov. Dielectric properties of Polycrystalline mixed nickel zinc ferrites. *Materials Letters.* 1994;40(45):3169-3176.
- [26]. Ravinder and K. Vijaya Kumar. Dielectric behavior of erbium substituted Mn-Zn ferrites. *Bull. Matter. Sc.* 2001;24(5):505-509.
- [27]. M. George, S. S. Nair, A. M. John, P. A. Joy, M. R. Anantharaman. Structural, magnetic and electrical properties of the sol gel prepared Li_{0.5}Fe_{2.5}O₄ fine particles. *Journal of Physics D: Applied Physics.* 2006;39:900-910.
- [28]. K. Arora, M. Sharma, R. Kumari, V.S. Jaswan and P. Kumar. Synthesis, Characterization and Magnetic Studies of α -Fe₂O₃ Nanoparticles. *Journal of Nanotechnology.* 2014;(2014):1-7.

Toijam Suma Chanu. " Green synthesis of Fe₂O₃ nanoparticles using Piper betle leaf and its characterization." *IOSR Journal of Applied Physics (IOSR-JAP)* , vol. 10, no. 5, 2018, pp. 32-38